Title page

Induced expression of Toll-like receptor 9 in peritubular capillary endothelium correlates with the progression of tubulointerstitial lesions in autoimmune disease-prone mice

Md. Abdul Masum[1, 2], Osamu Ichii[1, *], Yaser Hosny Ali ELewa[1, 3], and Yasuhiro Kon[1]

[1]Laboratory of Anatomy, Department of Basic Veterinary Sciences, Faculty of Veterinary Medicine, Hokkaido University, Sapporo, Japan

[2]Department of Anatomy, Histology and Physiology, Faculty of Animal Science and Veterinary Medicine, Sher-e-Bangla Agricultural University, Dhaka, Bangladesh

[3]Department of Histology, Faculty of Veterinary Medicine, Zagazig University, Zagazig, Egypt

*Corresponding Author:

Dr. Osamu Ichii,

Laboratory of Anatomy, Department of Basic Veterinary Sciences, Faculty of Veterinary Medicine, Hokkaido University, Kita 18, Nishi 9, Kita-ku, Sapporo 060-0818, Japan

Email: ichi-o@vetmed.hokudai.ac.jp

Tel: +81-11-706-5189, Fax: +81-11-706-5189

Abstract

Background: Toll-like receptor (Tlr) 9 is capable of recognizing exogenous and/or endogenous nucleic acids and plays a crucial role in innate and adaptive immunity. Recently, we showed that Tlr9 is overexpressed in podocytes, a component of the blood-urine barrier (BUB), in glomeruli of autoimmune glomerulonephritis (AGN) model mice. This study investigated the activation of peritubular capillary (PTC) endothelial cells (ECs), a component of the BUB in the tubulointerstitium, through overexpressing Tlr9, and the subsequent development of tubulointerstitial lesions (TILs) in AGN model mice.

Methods: Lupus-prone BXSB/MpJ-Yaa (Yaa) and BXSB/MpJ (BXSB) mice were used as an AGN model and control, respectively. In addition to histopathological and ultrastructural techniques, protein and mRNA levels were also evaluated. The relationship between Tlr9 and TIL indices was analyzed by statistical correlation analysis.

Results: Yaa mice developed TILs and showed strong Tlr9 mRNA expression in PTC ECs at 24 weeks (wks) of age. However, BXSB mice showed no TIL but faint expression of Tlr9 mRNA at 8 and 24 wks of age. Tlr9 protein localization on PTC was almost absent in BXSB mice at both ages but intense expression was found in Yaa mice only at 24 wks of age. Relative mRNA expression of *Tlr9* and its putative downstream cytokines, including interleukin 1 beta (*Il1b*), *Il6*, interferon gamma (*Ifng*), and tumor necrosis factor alpha (*Tnf*) was markedly increased in isolated tubulointerstitium from Yaa mice at 24 wks of age. Furthermore, electron microscopy examination revealed PTC injury and TIL in Yaa mice at 24 wks. The expression level of *Tlr9* in the tubulointerstitium was

correlated with inflammatory cells in TILs, injured PTC, *Ilb* and *Tnf* expression, and damaged tubules ($P < 0.05$ and 0.01).

Conclusion: Induced expression of *Tlr9* in ECs correlates with PTC injury and the development of TILs in lupus-prone AGN model mice.

Keywords

Toll-like receptor 9, peritubular capillary, tubulointerstitial lesions, autoimmune glomerulonephritis, BXSB/MpJ-Yaa mice.

Running title: Tlr9 in PTC correlates tubulointerstitial lesions.

Introduction

Chronic kidney disease (CKD) affects 22% of human adults in Japan, and 10–13% of the global population (1, 2). Most forms of CKD progress to either end-stage glomerulosclerosis or tubulointerstitial fibrosis (3). Therefore, CKD is a serious public health problem throughout the world, as it is associated with end-stage renal disease (ESRD), cardiovascular complications, and requires dialysis (4).

Though a variety of conditions, including infiltration of B-, T-cells, and macrophages, can lead to CKD in human and mice, the final common pathway of renal damage involves interstitial fibrosis, injury, and/or loss of renal tubules and peritubular capillaries (PTCs) (2, 5).

PTCs in the kidney are essential for regulating renal function and hemodynamics (6). PTC endothelial cells (ECs) also play a crucial role in expressing specific chemokines that control T-cell and monocyte recruitment during inflammation in experimental animals (7, 8). Importantly, ECs are being gradually recognized as active participants in the host's innate immune response to infection and injury. The engagement of endothelial innate immune receptors with host-derived agonists upregulates the expression of specific cytokines and chemokines, and increases the binding of neutrophils to the endothelium (9). ECs have been shown to express Toll-like receptors (Tlrs) that are activated in response to stimuli within the bloodstream, including pathogens and damage signals.

Inappropriate endothelial activation through Tlrs contributes to tissue damage during autoimmune and inflammatory diseases in human and murine disease models (10).

Tlrs act as sentinel receptors for the mammalian innate immune system and various studies have shown that Tlrs are expressed in intrinsic renal cells (11, 12). Particularly, *Tlr5* and *Tlr11* are expressed in tubular epithelial cells, and Tlrs also play an important role in urinary tract infections in mice (13, 14). The activation of different members of the Tlr family in tubular epithelial cells also contributes to the progression of kidney ischemia-reperfusion injury and subsequent renal fibrosis in human and mice (15).

However, among the members of Tlr family, Tlr9 shows the most variability both in expression and its role in the development of kidney diseases. A previous study showed Tlr9 expression in the tubulointerstitium and glomerulus of human patients with renal disease, but only in the tubulointerstitium of normal kidney (16). Machida *et al.*, showed that *Tlr9* is expressed on the podocytes of children with active lupus nephritis whereas *Tlr9* expression was also found in the glomerular capillary endothelium of patients with bacterial CpG-DNA-induced glomerulonephritis (17, 18). Therefore, *Tlr9* expression is not restricted only to antigen-presenting cells but also to murine endothelial cells (19, 20), human dermal microvascular endothelium (21), podocytes (17), and tubulointerstitium (13, 14), and it plays a crucial role in infectious and autoimmune responses. However, the role of Tlr9 in the development of tubulointerstitial lesions (TILs) has remained unclear.

Lupus-prone BXSB/MpJ-Yaa (Yaa) mice are generally used as the animal model of autoimmune glomerulonephritis (AGN). Importantly, male Yaa mice show more severe glomerular lesions (GLs) than females because of a mutation called the Y-linked autoimmune acceleration (Yaa) (22, 23). The Yaa locus contains approximately 19 protein-coding genes including *Tlr7* and *Tlr8* (22, 23). We also demonstrated that overexpression of *Tlr8* on the Yaa locus and *Tlr9* on the autosome were observed in podocytes, and their expression correlates with the progression of GL of AGN in Yaa mice (24, 25). Further, our previous studies have shown a close relationship with the number of glomerular capillaries and severity of GLs in Yaa mice (5). Importantly, these mice also developed TILs at a later stage. However, the mechanism of TIL development, especially the pathological correlations with Tlr expression, has not been fully elucidated yet.

In this study, we showed that *Tlr9* was expressed in injured PTCs of Yaa mice at 24 weeks (wks) of age. Moreover, *Tlr9* expression was correlated with TILs, indicating that de novo expression of *Tlr9* was related with PTC injury and subsequent development of TILs in AGN.

Materials and Methods

Ethical statements and maintenance of experimental animals

All experiments using mice were approved by the Institutional Animal Care and Use Committee of the Faculty of Veterinary Medicine, Hokkaido University (approval No. 13-0032, 16-0124). The authors adhered to the "Guide for the Care and Use of Laboratory Animals of Hokkaido University, Faculty of Veterinary Medicine," approved by the Association for Assessment and Accreditation of Laboratory Animal Care International throughout the experiments. Six-week-old male BXSB/MpJ (BXSB), Yaa, MRL/MpJ (MRL), and MRL/MpJ-lpr (lpr) mice were purchased from Japan SLC Inc. (Hamamatsu, Japan) and maintained under specific pathogen-free conditions. Twenty-four-week-old Yaa and lpr mice were designated as the AGN model.

Sample collection and preparation

Mice were anesthetized with a mixture of 0.3 mg/kg medetomidine (Kyoritsu Seiyaku, Tokyo, Japan), 5 mg/kg butorphanol (Meiji Seika Pharma, Tokyo, Japan), and 4 mg/kg midazolam (Astellas Pharma, Tokyo, Japan). The kidneys were cut into small slices and fixed in 10% neutral buffered formalin (NBF), 4% paraformaldehyde (PFA), or 2.5% glutaraldehyde (GTA) in 0.1 M phosphate buffer (PB) for routine histopathological analysis, immunostaining, and electron microscopy analysis, respectively. Kidney slices were fixed with 4% PFA for 2 hours followed by treatment with 30% sucrose and were then snap frozen in optimum cutting medium. To visualize

the vascular structures, the perfusion of Microfil (Flow Tech, Inc. Massachusetts, USA) throughout mouse hearts was performed according to our previously described methods (5).

Histopathological examination

The tissue sections were stained with periodic acid Schiff-hematoxylin (PAS-H) for histopathological analysis. Immunodetection of target cell markers was performed using kidney specimens fixed with PFA; details are listed in Supplementary Table 1. Briefly, deparaffinization and antigen retrieval was followed by submerging tissue sections in methanol containing 3% H_2O_2 for 20 min at room temperature and blocked with normal goat or donkey serum. Sections were incubated with primary antibody overnight at 4°C followed by incubation with the respective secondary antibodies at room temperature for 30 min: Alexa Fluor 546-labeled donkey anti-mouse IgG (Life Technologies, Yokohama, Japan) or Alexa Fluor 488-labeled donkey anti-rabbit IgG (Life Technologies, Yokohama, Japan). The sections were examined under an All-in-One Fluorescence Microscope BZ-X710 (Keyence, Osaka, Japan).

For immunohistochemistry, the sections were incubated with the appropriate biotinylated secondary antibody for 30 min, then with streptavidin-horseradish peroxidase (SABPO kit; Nichirei, Tokyo, Japan) for another 30 min, followed by incubation with 3,3-diaminobenzidine tetrahydrochloride-H_2O_2 solution. Finally, the

sections were counterstained with hematoxylin, dehydrated in an ascending series of alcohol solutions, and cleared with xylene.

In situ hybridization

A formalin-fixed paraffin-embedded RNAscope 2.5 assay was used for *in situ* hybridization in the tubulointerstitium. NBF-fixed paraffin-embedded kidney specimens were sliced into 5 μm-thick sections, air-dried overnight, and then baked in an oven for 1 h at 60°C. All procedures for *in situ* hybridization were performed according to the manufacturer's instructions for the RNAscope 2.5 HD Reagent Kit-RED (Advanced Cell Diagnostics, Inc., Hayward, CA, USA). RNAscope Target Probe-Mm-Tlr9, Mouse (Cat. No. 468281; Advanced Cell Diagnostics, Inc., Hayward, CA, USA), RNAscope positive control probe-Mm-Polr2a (Cat. No. 312471; Advanced Cell Diagnostics, Inc., Hayward, CA, USA), and RNAscope negative control probe-DapB (Cat. No. 310043; Advanced Cell Diagnostics, Inc., Hayward, CA, USA) was used according to the manufacturer's instructions for *in situ* hybridization.

Scanning electron microscopy (SEM) and modified SEM (mSEM)

For routine SEM, slices of GTA-fixed kidney were treated with tannic acid and post-fixed with 1% osmium tetroxide (OsO_4). The specimens were dehydrated and dried using an HCP-2 critical point dryer (Hitachi, Tokyo, Japan). The specimens were sputter-coated for 60 s with a Hitachi E-1030 ion sputter coater (Hitachi, Tokyo, Japan). Kidney sections were examined using an S-4100 SEM with an accelerating voltage of 10 kV. We

also used our previously described mSEM technique to examine the ultrastructure of the tubulointerstitium (26).

Histoplanimetry

Digital images randomly selected over 30 glomeruli or 30 tubulointerstitial areas from each mouse were acquired at high magnification (400×) using a BZ-X710 fluorescence microscope (Keyence). The number of $B220^+$ B-cells, $CD3^+$ T-cells, and $Iba1^+$ macrophages observed in the digital images of glomeruli were counted manually.

In addition to inflammatory cells, IL-1F6/IL-36^+ tubules were detected in the tubulointerstitium, as its immunoexpression signifies renal tubule damage which is also correlated with TILs and injured capillaries (5, 27). The numbers of $B220^+$ B-cells, $CD3^+$ T-cells, $Iba1^+$ macrophages, $CD31^+$ PTCs, $Tlr9^+$ PTCs, and IL-1F6/IL-$36\alpha^+$ damaged tubules in the digital images of the tubulointerstitium were assessed using a BZ-X Analyzer (Keyence). One hundred PTCs were selected randomly from each mouse using images obtained from modified scanning electron microscopy (mSEM). Among these, PTCs showing EC thickening with loss of fenestration as well as irregular and narrow capillary lumina were considered injured PTCs.

Laser microdissection (LMD), reverse transcription, and real-time PCR

Frozen sections were cut at 5-μm thickness and stained with toluidine blue. First, all glomeruli were removed from a kidney section by LMD using a MicroBeam Rel.4.2 (Carl Zeiss; Oberkochen, Germany). Whole kidney sections lacking glomeruli were

collected manually for further analysis from each mouse. Total RNA from dissected samples was isolated using a miRNeasy Micro Kit (Qiagen). Complementary DNA (cDNA) was synthesized from total RNA from dissected tubulointerstitium by reverse transcription by using ReverTra Ace qPCR RT Master Mix with gDNA Remover (Toyobo, Osaka, Japan). cDNA was used in real-time PCR with THUNDERBIRD SYBR qPCR mix (Toyobo) and a CFX Connect Real-Time PCR Detection System (Bio-Rad Laboratories, Inc., Tokyo, Japan). Gene expression in the tubulointerstitium was normalized to the expression of ß-actin (*Actb*). The primer pairs are shown in Supplementary Table 2.

Statistical analysis

The results were expressed as the mean ± standard error. The results were statistically analyzed using a nonparametric Mann-Whitney U-test ($P < 0.05$). The Kruskal-Wallis test was used to compare three or more populations, and multiple comparisons were performed using Scheffe's method when significant differences were observed ($P < 0.05$). The correlation was analyzed using Spearman's rank correlation test ($P < 0.05$).

Results

GLs and TILs in AGN model mice

Renal histopathology was examined in kidney sections from Yaa mice and their respective control BXSB mice at 8 and 24 wks of age (Fig. 1A-D). In control BXSB mice, no GLs or TILs were found at either age examined (Fig. 1A and C). However, Yaa mice showed no GLs and TILs at 8 wks of age but lesions were clearly found at 24 wks of age characterized by glomerular hypertrophy, increase in glomerular cell number, dilatation of tubules, presence of urinary cast in tubules, and infiltrating cells in tubulointerstitial spaces (Fig. 1B and D). Higher numbers of $B220^+$ B-cells, $CD3^+$ T-cells, and $Iba1^+$ macrophages were found in GLs and TILs of Yaa mice at 24 wks of age compared to those of Yaa mice at 8 wks of age and BXSB mice at both ages examined (Fig. 1E and F). These results indicate that Yaa mice developed GLs as well as TILs at 24 wks of age.

Normal distribution of PTCs in AGN model mice

Our previous study showed that number of PTCs decreased in a mouse model of TIL by unilateral ureter obstruction and their number related with TIL severity (5). As AGN model mice clearly showed TILs at 24 wks of age in the present study, we examined the distribution of PTCs at this age and found a normal distribution of $CD31^+$ PTCs (Supplementary Fig. 1). Further, the number of $CD31^+$ PTCs tended to be decreased in Yaa mice compared with BXSB mice, but no significant difference was observed (Supplementary Fig. 1). We also examined the distribution of PTCs in Microfil-perfused

kidney sections, and there was no significant difference between BXSB and Yaa mice (Supplementary Fig. 1).

mRNA expression and protein localization of Tlr9 in PTCs of AGN model mice

For *in situ* hybridization, no signals for *Tlr9* mRNA were detected in the tubulointerstitium of BXSB or Yaa mice at 8 wks of age (Fig. 2A and B). A slight number of signals for *Tlr9* mRNA was detected in the proximal tubules and PTCs of BXSB mice at 24 wks of age (Fig. 2C). However, strong signals for *Tlr9* mRNA were detected in PTCs of Yaa mice at 24 wks of age (Fig. 2D). As also found in our previous study (25), podocytes exhibited *Tlr9* expression (Supplementary Fig. 2). There was no or scant Tlr9 protein localization in PTCs of BXSB mice at both ages and Yaa mice at 8 wks of age (Fig. 2E-G). However, Tlr9 protein was abundantly localized in the cytoplasm of PTCs of Yaa mice at 24 wks of age (Fig. 2H). Tlr9-positive reactions were also detected in the podocytes of Yaa mice at 24 wks of age (Supplementary Fig. 2), as shown in our previous study (25). To examine the effect of *Yaa* mutation on Tlr9 expression in PTCs of Yaa mice, Tlr9 protein localization was also examined in another AGN model, lpr mice. Similar to the results in BXSB and Yaa mice, the respective control MRL showed no Tlr9 protein localization but intense reaction was found in PTCs of kidneys from lpr mice (Supplementary Fig. 3). Tlr9 immunoreaction was also confirmed in the spleens of 24 week-old Yaa mice (Supplementary Fig. 3). The percentage of $Tlr9^+$ PTCs was significantly higher in Yaa mice at 24 wks of age compared to that in other examined mice at both ages (Fig. 2I).

Expression of Tlr9 and its downstream cytokines in kidney tubulointerstitium

As shown in Fig. 3, we examined mRNA expression in the tubulointerstitium by using LMD following real-time PCR at 24 wks of age. mRNA expression of *Tlr9* was significantly higher in Yaa mice than that in BXSB mice. Further, levels of its downstream cytokines (28) including interleukin 1 beta (*Il1b*), *Il6*, interferon gamma (*Ifng*), and tumor necrosis factor alpha (*Tnf*) also tended to be upregulated in the tubulointerstitium of Yaa mouse kidneys compare to levels in BXSB mice, and significant differences were observed for *Il1b* and *Il6*.

PTC injury in AGN model mice

We examined ultrastructural injury of PTCs in all examined mouse kidneys. mSEM showed that BXSB and Yaa mice at 8 wks of age exhibited preserved normal PTC structures (Fig. 4A and B). BXSB mice at 24 wks of age showed normal PTCs but Yaa mice at the same age showed PTC injury characterized by thickening of ECs, loss of fenestration, and irregular capillary lumina (Fig. 4C and D). Yaa mice also showed wide tubulointerstitial spaces, indicating edema, with infiltrating immune cells. For the standard SEM method, BXSB mice at both ages and Yaa at 8 wks of age showed well-preserved PTC lumina (Fig. 4E-G), but Yaa mice showed loss of endothelial fenestration at 24 wks of age (Fig. 4H). A greater percentage of injured PTCs was found in Yaa mice at 24 wks of age compared to other examined mice at both ages (Fig. 4I).

Tubular injury in AGN model mice

In our previous study, increased numbers of IL-1F6/IL-36α$^+$ distal tubules were found in injured kidneys, which also related with TIL (27). Moreover, IL-1F6/IL-36α$^+$ tubules were correlated with EC injury and PTC loss (5). BXSB and Yaa mice at 8 wks of age showed no IL-1F6/IL-36α$^+$ tubules (Fig. 5A and B). BXSB mice at 24 wks of age showed normal tubules, but Yaa mice at the same age showed abundant IL-1F6/IL-36α$^+$ tubules (Fig. 5C and D). Greater numbers of IL-1F6/IL-36α$^+$ damaged tubules were found in Yaa mice at 24 wks of age compared to those of 8 wks of Yaa mice and both ages of BXSB mice (Fig. 5E). mSEM analysis also revealed tubular dilatation, flattened tubular epithelium, wide tubulointerstitial spaces, and misshapen capillary lumina (Fig. 5F-I). These data indicated that PTC injury was accompanied by tubular injury in Yaa mice at 24 wks of age.

Correlation among the indices of renal Tlr9 expression, PTC injuries, and TILs

We analyzed the statistical correlation among renal *Tlr9* expression, PTC injuries, and TILs by using the parameters obtained from all animals (Table 1). *Tlr9* expression level in tubulointerstitium examined by LMD was positively and significantly correlated with immune cell infiltration into TILs, mRNA expression of proinflammatory cytokines (*Il1b, Tnf*) in the tubulointerstitium, the percentage of injured PTCs examined by mSEM, and the number of IL-1F6/IL-36α$^+$ tubules. The percentage of Tlr9$^+$ PTCs and injured PTCs examined by immunostaining and mSEM, respectively, also showed a similar

279 positive and significant tendency toward correlation, except for the parameters of
280 macrophage infiltration into TILs and mRNA expression of *Il6* and *Ifng* in
281 tubulointerstitium. The number of IL-1F6/IL-36α^{+} tubules was positively and
282 significantly correlated with immune cell infiltration into TILs, mRNA expression of
283 proinflammatory cytokines (except *Ifng*) in the tubulointerstitium, the percentage of
284 injured PTCs examined by mSEM, and the percentage of Tlr9^{+} PTCs.

285

Discussion

In the present study, we have introduced a potential role of the innate immune system through activation of Tlr9 in PTC ECs in AGN model mice. We showed de novo expression of Tlr9 in PTC ECs for the first time and subsequent injury. In addition, we also elucidated the contribution of this injured PTC to the development of TILs in AGN.

Chronic GLs are thought to be converted into TILs by overfiltration of plasma proteins, inflammatory cytokines, or hypoxia (29). Therefore, AGN can chronically progress to ESRD through the interstitial fibrosis associated with the injury of renal tubules and PTCs. Importantly, the number of damaged tubules increased with immune cell infiltration and elevated expression of proinflammatory cytokines in the tubulointerstitium of AGN model mice. In glomerulonephritis, resident glomerular cells are damaged, and they secrete inflammatory cytokines that can activate interstitial cells and induce inflammatory cell infiltration (30). Previously, we showed that injury and loss of glomerular capillaries negatively correlated with the development of GLs. Importantly, the efferent arterioles from the glomerulus allow the PTC to branch to the tubulointerstitium. Further, as altered renal vasculature in the kidney leads to hypoxia which results in renal inflammation in humans and experimental animals (6, 31), in the present study, we attempted to determine the correlation between PTC injury and TILs in AGN model mice. Importantly, the number of PTCs was not significantly altered in AGN model mice, but the ultrastructural changes characterized by narrow and irregular of PTC lumina, EC thickening with loss of fenestration, and EC activation or detachment with

peritubular infiltration of immune cells were clearly induced in PTCs in AGN model mice. Furthermore, a significant positive correlation was found between PTC injury and TILs. Therefore, we considered that PTC injury was accompanied with the development of AGN and inflammatory TILs, and injured ECs of PTC in AGN caused local hypoxia which can contribute to TIL development.

ECs are now considered active members of innate immunity that participate in the innate immune response to infection and injury. Tlrs, members of the innate immune response, are selectively expressed in ECs. Among Tlrs, *Tlr9* is expressed in different ECs and causes tissue damage (20, 32). Moreover, our previous study showed that overexpressing *Tlr8* and *Tlr9* in glomerular podocytes correlated with the progression of AGN in mice (24, 25). Podocytes are crucial cells for maintaining the barrier between renal tissues and the blood stream, known as the BUB. Similarly, renal tubular epithelial cells and ECs of PTC have important roles in the barrier between renal tissues and the bloodstream by reabsorbing filtrate components into the PTC and trafficking leukocytes from the bloodstream to the extravascular space, respectively (33, 34). Therefore, similar to podocytes, we hypothesized that tubulointerstitium like PTC ECs or tubular epithelium would participate in the innate immune response by expressing Tlrs. As expected, in the present study, we found that *Tlr9* mRNA was expressed in podocytes as well as ECs of PTCs in Yaa mice. We also demonstrated that expression of *Tlr9* and its downstream cytokines *Il1b*, *Il6*, *Ifng*, and *Tnf*, was induced by activation of the NF-kB pathway (28) in the tubulointerstitium of AGN mice. From these results, similar to the GL pathogenesis

via Tlr9-NF-kB (25), we concluded that this pathway also plays an important role in the progression of TIL in AGN model mice.

*Tlr9 e*xpression was observed only in AGN model mice at 24 wks of age, but not in control and younger mice. The duplicated Yaa locus of Yaa mice contains approximately 19 protein-coding genes including Tlr7 and Tlr8 (22, 23), whereas *Tlr9* is located in the autosome. Further, this result was also confirmed by showing Tlr9 protein localization in PTC of another AGN mouse model, the lpr strain. Therefore, overexpression of *Tlr9* in PTC was not due to genomic factors, but systemic autoimmune disease condition would increase its expression. Importantly, Tlr9 is localized to the endosomes, and it can recognize internalized CpG-DNA from bacteria and DNA viruses (35) and host-derived nucleic acids (36). Interestingly, immune-complexes containing DNA internalized via Fc gamma receptor also seem to bind to Tlr9 in endosomes (37). Importantly, the serum level of anti-dsDNA autoantibodies is remarkably high in Yaa mice and lpr mice (25). Therefore, overexpression of *Tlr9* of ECs in PTCs might be needed to process the increased immune-complexes circulating in the bloodstream and/or reflected the increased endosomal activities in ECs. In fact, EC ultrastructural observations showed increased cytoplasm size. Taken together, the results suggest that Tlr9 participates in the progression of TILs as a modulator rather than an initiator by activating downstream inflammatory pathways.

The activation of ECs through Tlrs was also found in humans and experimental animals through prior inflammatory stimuli such as *Ifng*, *Tnf*, or *Ilb* (10, 32, 38). To

examine the response of ECs via Tlr9 by candidate ligands and/or cytokines, ex vivo analysis of ECs in PTCs from the kidney would be useful. However, the expression of Tlr family proteins depends on origin or location of ECs (34, 39). Although we isolated glomeruli by bead-circulation methods and demonstrated faint *Tlr9* expression in glomerular ECs with the combination of histological study (25), purifying the ECs in PTCs would be unrealistic methodologically. Therefore, we applied the correlation analysis between *Tlr9* expression and histopathological indices to estimate the function of Tlr9 in ECs of PTCs. The present statistical analysis revealed that *Tlr9* expression in tubulointerstitium was positively correlated with immune cell infiltration into TILs, mRNA expression of proinflammatory cytokines (*Il1b*, *Tnf*) in the tubulointerstitium, the percentage of injured PTCs examined by mSEM, and the number of IL-1F6/IL-36α+ tubules. These results suggest that PTC ECs activation through Tlr9 induces proinflammatory cytokine production, which enhances the injury of PTC ECs and tubules in an autocrine and paracrine manner.

Conclusion

In summary, we have demonstrated that EC Tlr9 leads to inflammatory cell recruitment into the tubulointerstitium and TILs in AGN. In addition, PTC injury and TILs were accompanied by GLs in AGN model mice, suggesting crosstalk between the glomerulus and tubulointerstitium during disease progression. However, critical details about the postulated series of events remain to be elucidated, such as more specific characterization of Tlr9 ligands that are induced in this model. The comparative

contribution of Tlr9 and other Tlrs would also be beneficial to elucidate a more complete picture of the development of TILs in AGN.

Funding

This study was supported by a Grant-in-Aid for Scientific Research to a Graduate Student from the Graduate School of Veterinary Medicine, Hokkaido University, Japan (Grant-in Aid FY 2017, PH36150001, Mr. Masum) and Kazato Research Grants (Dr. Ichii).

Acknowledgement

The authors thank to Dr. David P. Basile (Indiana University School of Medicine, Indiana, USA) for critical discussion and suggestions.

Declaration of interest

The authors declare that there were no competing of interests.

References

1. Nagata M, Ninomiya T, Doi Y, et al. Trends in the prevalence of chronic kidney disease and its risk factors in a general Japanese population: the Hisayama Study. *Nephrol Dial Transplant* 2010; 25: 2557–2564.
2. Kida Y, Tchao BN and Yamaguchi I. Peritubular capillary rarefaction: a new therapeutic target in chronic kidney disease. *Pediatr Nephrol* 2014; 29: 333–342.
3. Eddy AA. Molecular insights into renal interstitial fibrosis. *J Am Soc Nephrol* 1996; 7: 2495-2508.
4. Tonelli M, Wiebe N, Culleton B, et al. Chronic kidney disease and mortality risk: a systematic review. *J Am Soc Nephrol* 2006; 17: 2034-2047.
5. Masum MA, Ichii O, Elewa YHA, Nakamura T and Kon Y. Local CD34-positive capillaries decrease in mouse models of kidney disease associating with the severity of glomerular and tubulointerstitial lesions. *BMC Nephrol* 2017; 18(1): 280. doi: 10.1186/s12882-017-0694-3.
6. Ohashi R, Kitamura H and Yamanaka N. Peritubular capillary injury during the progression of experimental glomerulonephritis in rats. *J Am Soc Nephrol* 2000; 11: 47–56.
7. Panzer U, Steinmetz OM, Reinking RR, et al. Compartment-specific expression and function of the chemokine IP-10/ CXCL10 in a model of renal endothelial microvascular injury. *J Am Soc Nephrol* 2006; 17: 454–464.

8. Lim YC, Garcia-Cardena G, Allport JR, et al. Heterogeneity of endothelial cells from different organ sites in T-cell subset recruitment. *Am J Pathol* 2003; 162: 1591–601.
9. Hickey MJ and Kubes P. Intravascular immunity: the host-pathogen encounter in blood vessels. *Nat Rev Immunol* 2009; 9: 364-375.
10. Salvador B, Arranz A, Francisco S, et al. Modulation of endothelial function by Toll like receptors. *Pharmacol Res* 2016; 108: 46-56.
11. Baccala R, Gonzalez-Quintial R, Lawson BR, et al. Sensors of the innate immune system: their mode of action. *Nat Rev Rheumatol* 2009; 5: 448–456.
12. Garraud O and Cognasse F. Platelet Toll-like receptor expression: the link between "danger" ligands and inflammation. *Inflamm Allergy Drug Targets* 2010; 9: 322–333.
13. Andersen-Nissen E, Hawn TR, Smith KD, et al. Cutting edge: Tlr5-/- mice are more susceptible to Escherichia coli urinary tract infection. *J Immunol* 2007; 178: 4717–4720.
14. Zhang D, Zhang G, Hayden MS, et al. A toll-like receptor that prevents infection by uropathogenic bacteria. *Science* 2004; 303: 1522–1526.
15. Shigeoka AA, Holscher TD, King AJ, et al. TLR2 is constitutively expressed within the kidney and participates in ischemic renal injury through both MyD88-dependent and-independent pathways. *J Immunol* 2007; 178: 6252–6258.
16. Papadimitraki ED, Tzardi M, Bertsias G, Sotsiou E and Boumpas DT. Glomerular expression of toll-like receptor-9 in lupus nephritis but not in normal kidneys: implications for the amplification of the inflammatory response. *Lupus* 2009; 18: 831–835.

17. Machida H, Ito S, Hirose T, et al. Expression of Toll-like receptor 9 in renal podocytes in childhood-onset active and inactive lupus nephritis. *Nephrol Dial Transplant* 2010; 25: 2530–2537.
18. Anders HJ, Banas B, Linde Y, et al. Bacterial CpG-DNA aggravates glomerulonephritis: role of TLR9-mediated expression of chemokines and chemokine Receptors. *J Am Soc Nephrol* 2003; 14: 317–326.
19. Li J, Ma Z, Tang ZL, et al. CpG DNA-mediated immune response in pulmonary endothelial cells. *Am J Physiol* 2004; 287: L552–L558.
20. Martin-Armas M, Simon-Santamaria J, Pettersen I, et al. Toll-like receptor 9 (TLR9) is present in murine liver sinusoidal endothelial cells (LSEC) and mediates the effect of CpG-oligonucleotides. *J Hepatol* 2006; 44: 939–946.
21. Fitzner N, Clauberg S, Essmann F, et al. Human skin endothelial cells can express all 10 TLR genes and respond to respective ligands. *Clin Vaccine Immunol* 2008, 15: 138–146.
22. Santiago-Raber ML, Laporte C, Reininger L, Izui S. Genetic basis of murine lupus. *Autoimmun Rev* 2004; 3: 33–39.
23. Subramanian S, Tus K, Li QZ, et al. A Tlr7 translocation accelerates systemic autoimmunity in murine lupus. *Proc Natl Acad Sci USA* 2006; 103: 9970–9975.
24. Kimura J, Ichii O, Miyazono K, et al. Overexpression of toll-like receptor 8 correlates with the progression of podocyte injury in murine autoimmune glomerulonephritis. *Sci Rep* 2014; 4: 7290. doi: 10.1038/srep07290.

25. Masum MA, Ichii O, Elewa YHA, et al. Overexpression of Toll-like receptor 9 correlates with podocyte injury in a murine model of autoimmune membranoproliferative glomerulonephritis. *Autoimmunity* (Submitted, under revision).

26. Masum MA, Ichii O, Elewa YHA, et al. Modified scanning electron microscopy reveals pathological crosstalk between endothelial cells and podocytes in a murine model of membranoproliferative glomerulonephritis. *Sci Rep* 2018; 8: 10276. doi: 10.1038/s41598-018-28617-1.

27. Ichii O, Otsuka S, Sasaki N, et al. Local overexpression of interleukin-1 family, member 6 relates to the development of tubulointerstitial lesions. *Lab Invest* 2010; 90: 459–475.

28. Shirali AC and Goldstein DR. Tracking the Toll of Kidney Disease. *J Am Soc Nephrol* 2008; 19: 1444–1450.

29. Kriz W and LeHir M. Pathways to nephron loss starting from glomerular diseases: insights from animal models. *Kidney Int* 2005; 67: 404–419.

30. Pichler R, Giachelli C, Young B, et al. The pathogenesis of tubulointerstitial disease associated with glomerulonephritis: The glomerular cytokine theory. *Miner Electrolyte Metab* 1995; 21: 317–327.

31. Fine LG and Norman JT. Chronic hypoxia as a mechanism of progression of chronic kidney diseases: from hypothesis to novel therapeutics. *Kidney Int* 2008; 74: 867–872.

32. El Kebir D, Jozsef L, Pan W, Wang L and Filep JG. Bacterial DNA Activates Endothelial cells and promotes neutrophil adherence through TLR9 signaling. *J Immunol* 2009; 182: 4386–4394.

33. Vedula M, Alonso JL, Arnaout MA and Charest JL. A microfluidic renal proximal tubule with active reabsorptive function. *PLoS ONE* 2017; 12: e0184330. https://doi.org/10.1371/journal. pone.0184330.

34. Khakpour S, Wilhelmsen K and Hellman J. Vascular endothelial cell toll-like receptor pathways in sepsis. *Innate Immun* 2015; 21: 827–846.

35. Hemmi H, Takeuchi O, Kawai T, et al S. A Toll-like receptor recognizes bacterial DNA. *Nature* 2000; 408: 740–745

36. Saitoh S and Miyake K. Regulatory molecules required for nucleotide sensing Toll-like receptors. *Immunol Rev* 2009; 227: 32–43.

37. Means TK, Latz E, Hayashi F, et al. Human lupus autoantibody-DNA complexes activate DCs through cooperation of CD32 and TLR9. *J Clin Invest* 2005; 115: 404-417.

38. Sabry A, Sheashaa H, El-Husseini A, et al. Proinflammatory cytokines (Tnfalpha and IL-6) in Egyptian patients with SLE: its correlation with disease activity. *Cytokine* 2006; 35: 148–153

483 39. Opitz B, Eitel J, Meixenberger K and Suttorp N. Role of toll-like receptors, NOD-
484 like receptors and RIG-I-like receptors in endothelial cells and systemic infections.
485 *Thromb Haemost* 2009; 102: 1103–1109.

486

Figure 1. GLs and TILs in AGN model mice

(**A-D**) GLs and TILs in PAS-H stained sections obtained from BXSB and Yaa mice at 8 and 24 wks of age. BXSB mice show no lesions at 8 and 24 wks of age (A and C). Yaa mice show no lesions at 8 wks of age (B) but exhibited GLs at 24 wks (dashed area), and TILs characterized by dilated tubules (arrow) containing urinary cast (arrowhead) (D). Bars = 100μm.

(**E and F**) Number of infiltrating cells in kidneys from AGN model mice. Number of infiltrating B-, T-cells, and macrophages in glomerulus (E) and tubulointerstitium (F) of BXSB and Yaa mice at 8 and 24 wks of age. Values are mean ± s.e. *: Significant difference from the control in the same disease group, Mann-Whitney U test ($*p < 0.05$). # Significant difference from the other groups, Kruskal-Wallis test followed by Scheffe's method ($\#\#p < 0.01$). n = 4. GLs: Glomerular lesions, TILs: Tubulointerstitial lesions, AGN: autoimmune glomerulonephritis, PAS-H: periodic acid Schiff-hematoxylin, BXSB: BXSB/MpJ, Yaa: BXSB/MpJ-Yaa, wks: weeks and ND: not detected.

Figure 2. Expression and localization of Tlr9 in tubulointerstitium of AGN model mice

(**A and B**) In situ expression of Tlr9 mRNA in the tubulointerstitium of BXSB and Yaa mice at 8 wks of age as determined by in situ hybridization. There are no signals in the tubulointerstitium of BXSB (A) or Yaa mice (B) at 8 wks of age.

(**C and D**) In situ expression of Tlr9 mRNA in the tubulointerstitium of BXSB and Yaa mice at 24 wks of age as determined by in situ hybridization. There are a scant number of signals for the genes hybridized with the probe for Tlr9 mRNA in the PTC of control BXSB mice at 24 wks of age (C). There are numerous strong signals (arrows) for the genes hybridized with the probe for Tlr9 mRNA in the PTC of model mice (Yaa) at 24 wks of age (D). Bars = 50μm.

(**E and F**) Tlr9 protein localization in the tubulointerstitium of BXSB and Yaa mice at 8 wks of age as determined by immunofluorescence. There is no immunoexpression in the tubulointerstitium of BXSB (E) or Yaa mice (F) at 8 wks of age.

(**G and H**) Tlr9 protein localization in the tubulointerstitium of BXSB and Yaa mice at 24 wks of age as determined by immunofluorescence. There is no Tlr9 protein localization in the PTC of control BXSB mice at 24 wks of age (G). Tlr9 protein localized in the PTC of model mice (Yaa) at the same age (H). Bars = 50μm.

(**I**) Percentage of PTC showing Tlr9 protein localization in BXSB and Yaa mice at 8 and 24 wks of age. Values are mean ± s.e. *: Significant difference from the control in the same disease group, Mann-Whitney U test (**$p < 0.01$). # Significant difference from the other groups, Kruskal-Wallis test followed by Scheffe's method (##$p < 0.01$). n = 4. AGN: autoimmune glomerulonephritis, PTC: peritubular capillary, BXSB: BXSB/MpJ, Yaa: BXSB/MpJ-*Yaa*, wks: weeks, and ND: not detected.

Figure 3. Expression of *Tlr9* and its downstream factors in the tubulointerstitium of in AGN model mice

Relative mRNA expression of *Tlr9* and its downstream factors, including *Ilb*, *Il6, Ifng*, and *Tnf* in the tubulointerstitium isolated from BXSB and Yaa mice at 24 weeks of age; analysis was conducted by real-time PCR. The expression levels were normalized to the levels of *Actb*. Values are mean ± s.e. *Significantly different from BXSB mice at the same age (Mann-Whitney *U*-test, $P < 0.05$); n = 4. *Il1b*: interleukin 1 beta, *Il6*: interleukin 6, *Ifng*: interferon gamma, *Tnf*: tumor necrosis factor alpha, AGN: autoimmune glomerulonephritis, BXSB: BXSB/MpJ, Yaa: BXSB/MpJ-*Yaa*, and wks: weeks.

Figure 4. PTC injury in AGN model mice

(**A-D**) PTC injury in BXSB and Yaa mice at 8 and 24 wks of age as determined by mSEM. Normal PTC in BXSB mice at 8 and 24 wks of age (A and C). Yaa mice show normal PTC at 8 wks of age (B) but show thickening of endothelial cytoplasm with loss of fenestration at 24 wks (D). Bars = 5μm.

(**E-H**) Morphological changes of PTC lumen in BXSB and Yaa mice at 8 and 24 wks of age as determined by SEM. BXSB mice show normal PTC lumen at 8 and 24 wks of age (E and G). Yaa mice also show normal PTC lumen at 8 wks of age (F) but show loss of endothelial fenestration at 24 wks (H). Bars = 5μm.

(**I**) Percentage of injured PTCs in BXSB and Yaa mice at 8 and 24 wks of age. Values are mean ± s.e. *: Significant difference from the control in the same disease group, Mann-

Whitney *U* test ($^{**}p < 0.01$). $^{\#}$ Significant difference from the other groups, Kruskal-Wallis test followed by Scheffe's method ($^{\#\#}p < 0.01$). n = 4. mSEM: Modified scanning electron microscopy, SEM: Scanning electron microscopy, AGN: autoimmune glomerulonephritis, PTC: peritubular capillary, BXSB: BXSB/MpJ, Yaa: BXSB/MpJ-*Yaa*, wks: weeks and ND: not detected.

Figure 5. TILs in AGN model mice

(**A-D**) IL-1F6/IL-36α+ damaged tubules in tubulointerstitium of BXSB and Yaa mice at 8 and 24 wks of age as determined by immunohistochemistry. BXSB mice show no tubular injury at 8 and 24 wks of age (A and C). Yaa mice show no tubular injury at 8 wks of age (B) but show many IL-1F6/IL-36α+ damaged tubules in the tubulointerstitium at 24 wks (arrow) (D). Bars = 100μm.

(**E**) Number of IL-1F6/IL-36α+ damaged tubules in the tubulointerstitium of BXSB and Yaa mice at 8 and 24 wks of age. Values are mean ± s.e. *: Significant difference from the control in the same disease group, Mann-Whitney U test (**p < 0.01). # Significant difference from the other groups, Kruskal-Wallis test followed by Scheffe's method (##p < 0.01).

(**F-I**) TILs in BXSB and Yaa mice at 8 and 24 wks of age as determined by mSEM. BXSB mice show normal tubulointerstitium at 8 and 24 wks of age (F and H). Yaa also show normal tubulointerstitium at 8 wks of age (G) but show dilated tubules (arrow), edematous

567 tubulointerstitial space (arrowhead), and narrow PTC (empty arrowhead) at 24 wks (I).
568 Bars = 10μm. TILs: Tubulointerstitial lesions, mSEM: Modified scanning electron
569 microscopy, AGN: autoimmune glomerulonephritis, PTC: peritubular capillary, BXSB:
570 BXSB/MpJ, Yaa: BXSB/MpJ-Yaa, wks: weeks, and ND: not detected.

Figure 1

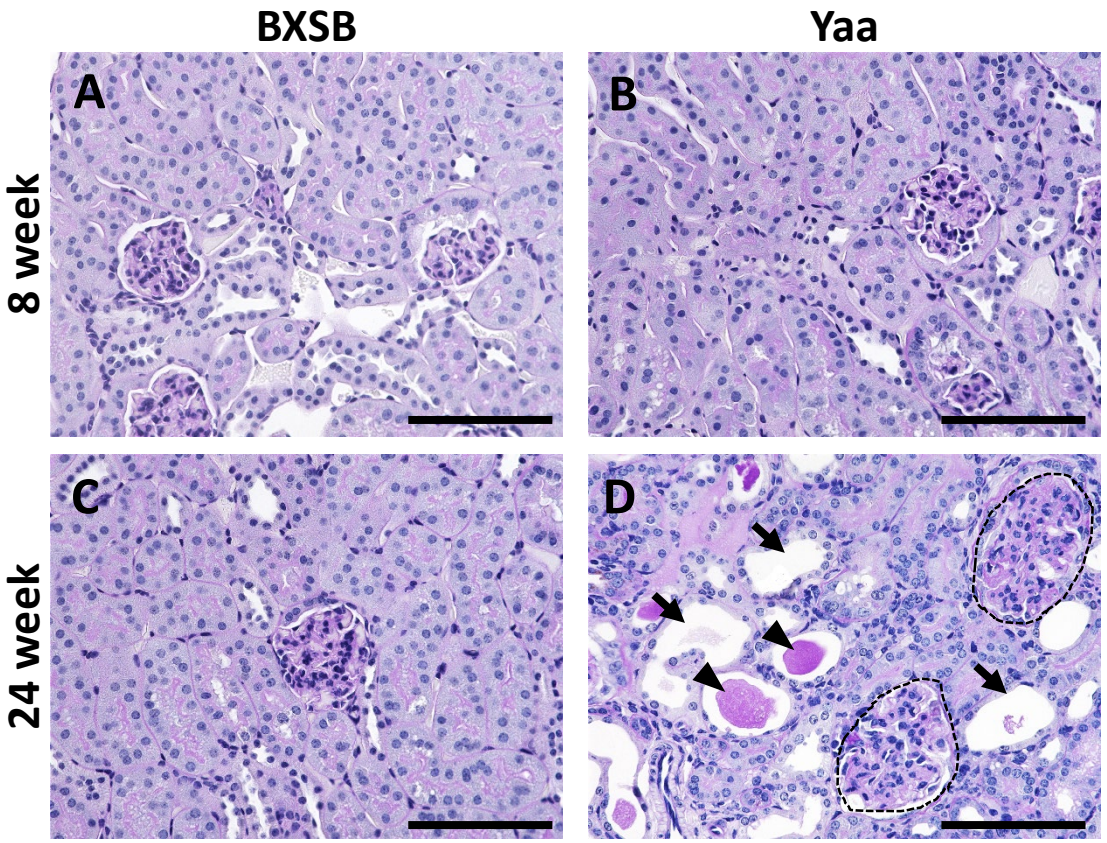
BXSB
Yaa
A
B
8 week
C
D
24 week

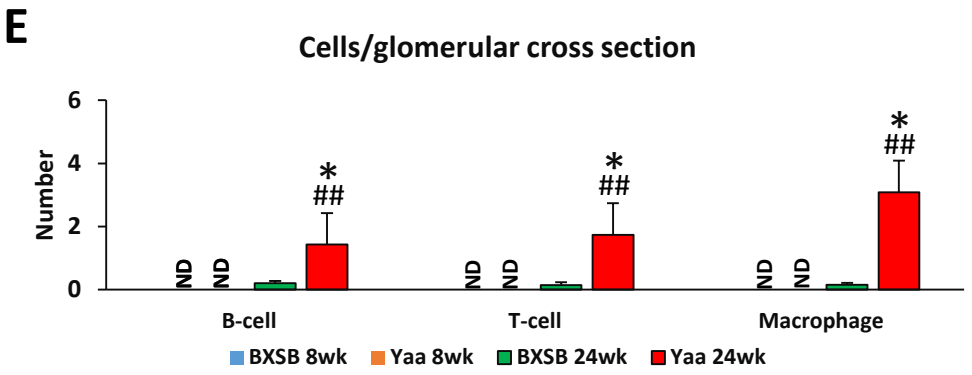
E
Cells/glomerular cross section
Number
6
4
2
0
ND
ND
*
##
B-cell
T-cell
Macrophage
BXSB 8wk
Yaa 8wk
BXSB 24wk
Yaa 24wk

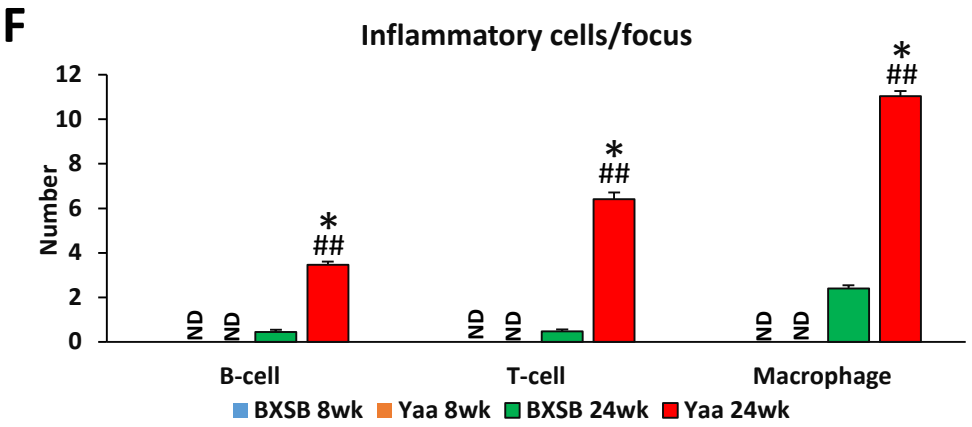
F
Inflammatory cells/focus
Number
12
10
8
6
4
2
0
ND
ND
*
##
B-cell
T-cell
Macrophage
BXSB 8wk
Yaa 8wk
BXSB 24wk
Yaa 24wk

Figure 2

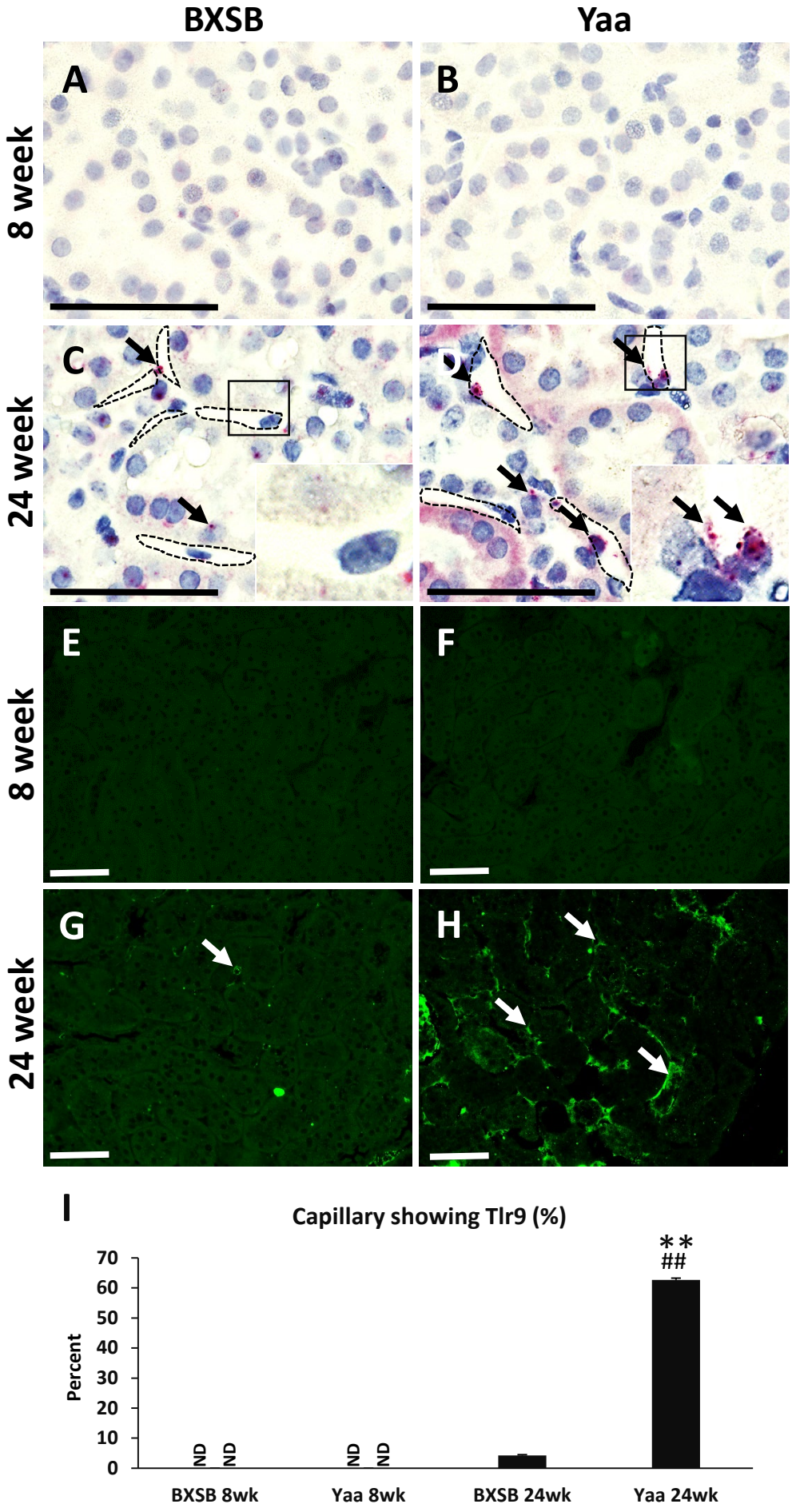
BXSB
Yaa
A
B
8 week
C
D
24 week
E
F
8 week
G
H
24 week
I
Capillary showing Tlr9 (%)
Percent
70
60
50
40
30
20
10
0
ND
ND
ND
ND
**
##
BXSB 8wk
Yaa 8wk
BXSB 24wk
Yaa 24wk

Figure 3

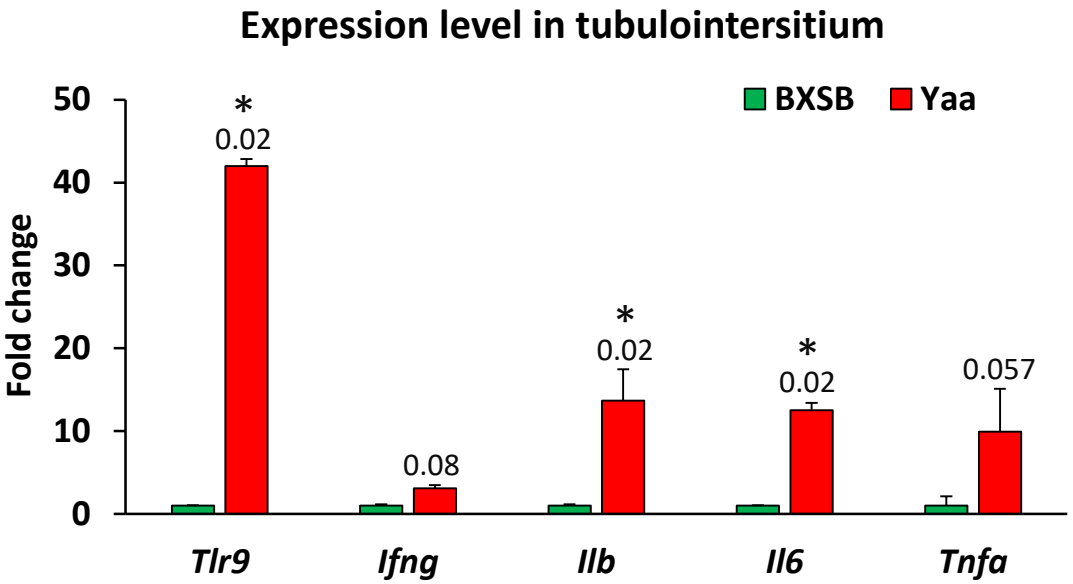
Expression level in tubulointersitium
BXSB
Yaa
Fold change
50
40
30
20
10
0
*
0.02
0.08
*
0.02
*
0.02
0.057
Tlr9
Ifng
Ilb
Il6
Tnfa

Figure 4

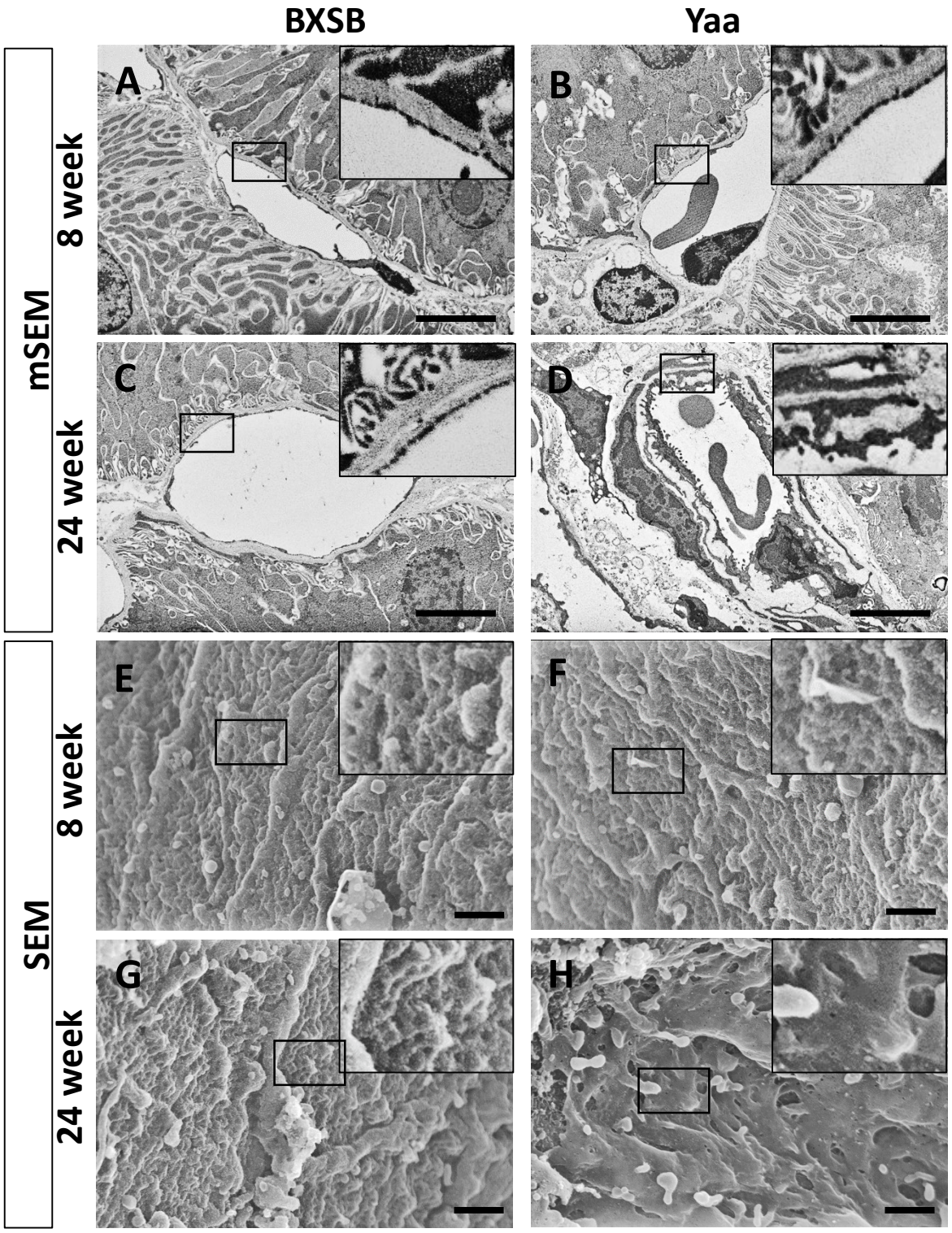
BXSB
Yaa
mSEM
SEM
8 week
24 week
A
B
C
D
E
F
G
H

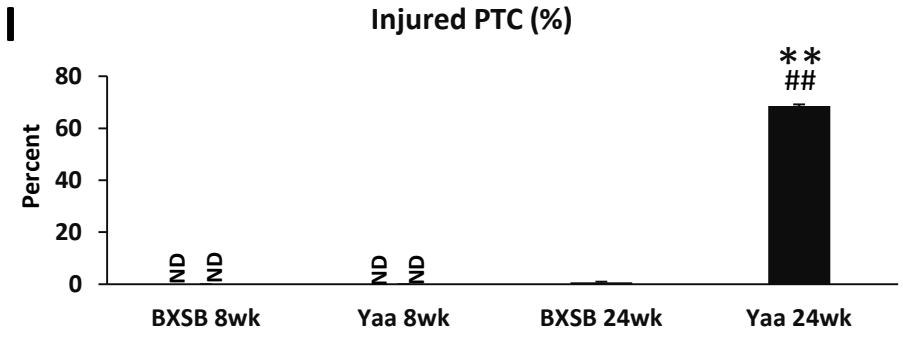
I
Injured PTC (%)
Percent
80
60
40
20
0
ND
ND
ND
ND
**
##
BXSB 8wk
Yaa 8wk
BXSB 24wk
Yaa 24wk

Figure 5

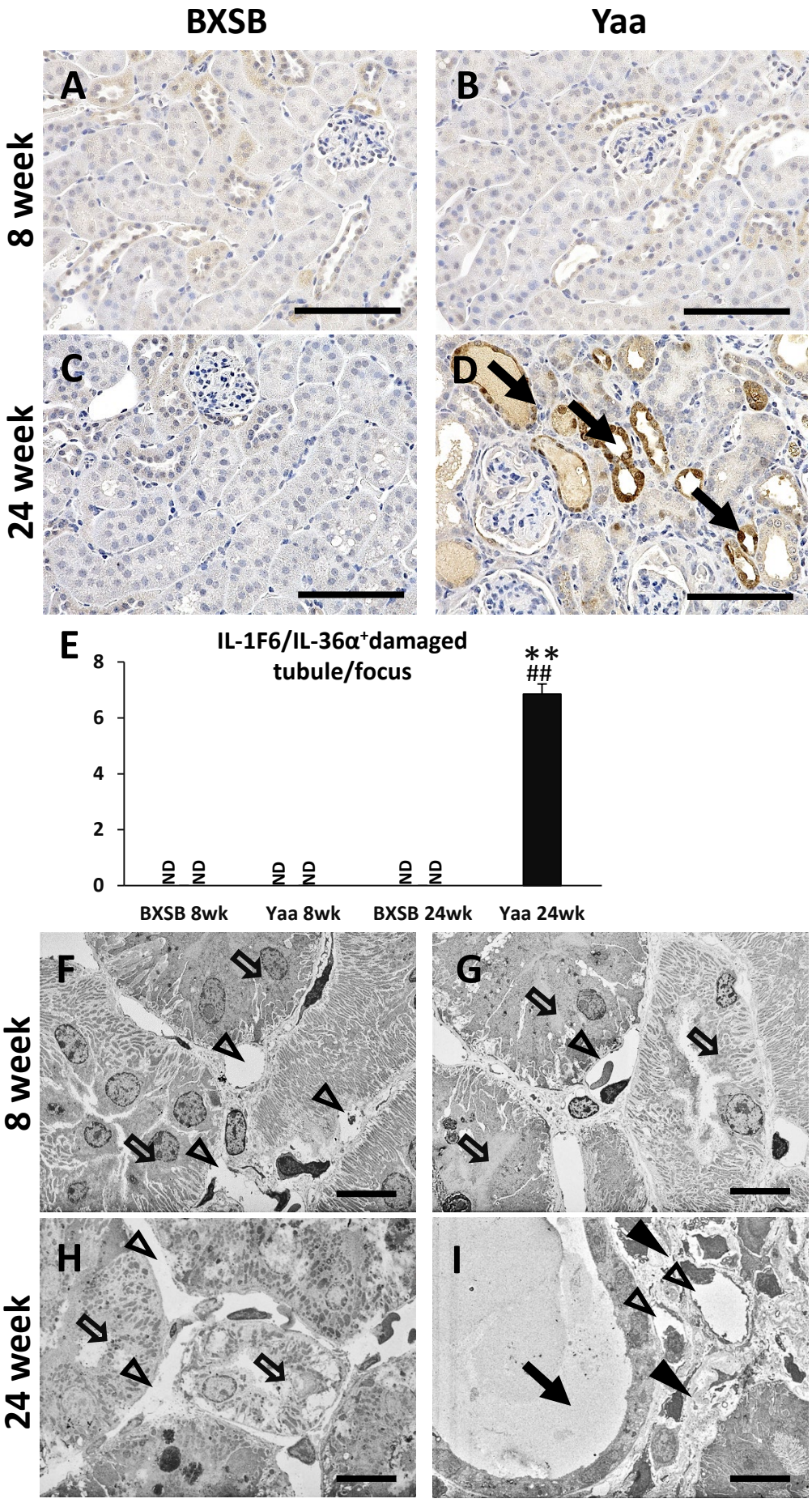
BXSB
Yaa
8 week
24 week
A
B
C
D
E
IL-1F6/IL-36α⁺damaged tubule/focus
8
6
4
2
0
ND
ND
ND
ND
ND
ND
**
##
BXSB 8wk
Yaa 8wk
BXSB 24wk
Yaa 24wk
F
G
H
I

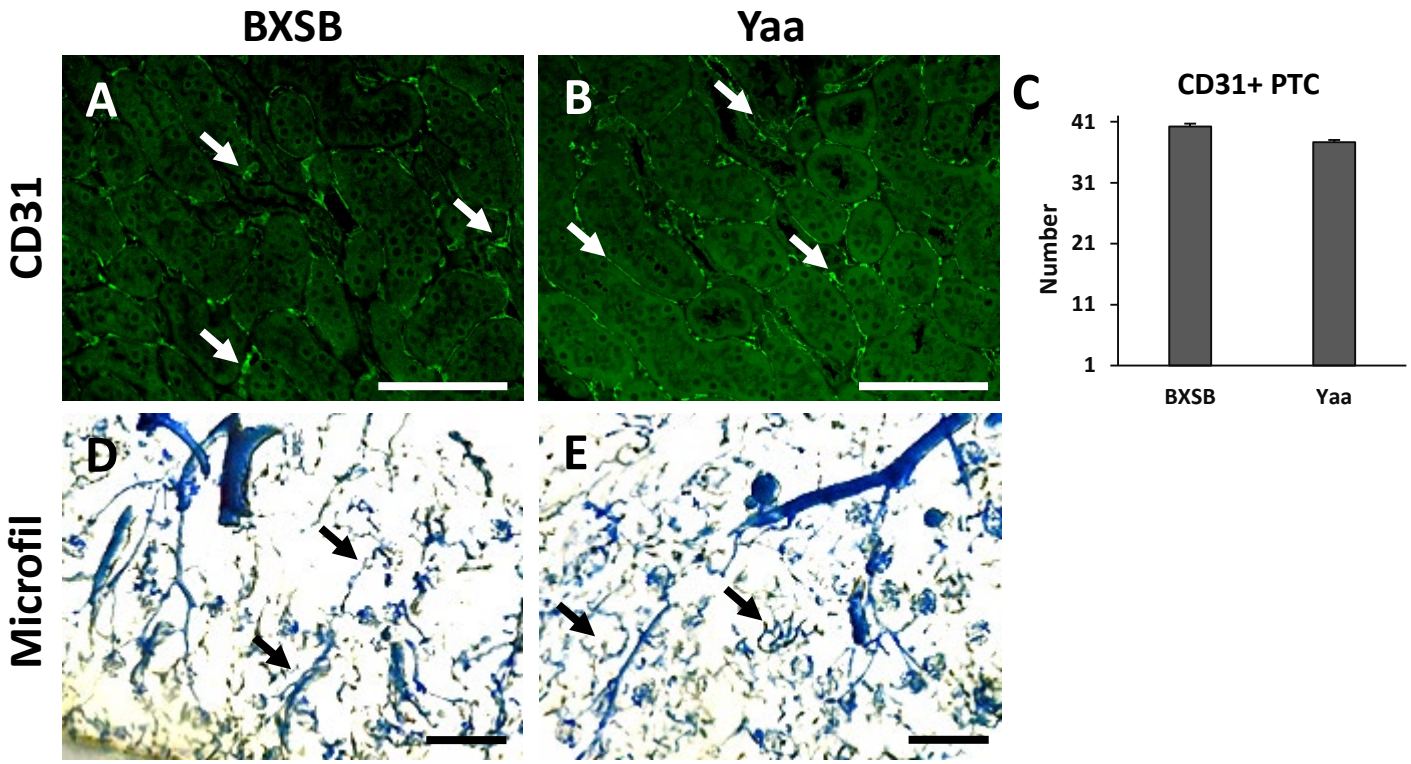

Supplementary Figure 1. Distribution of PTC in AGN model mice

(**A and B**) Distribution of $CD31^+$ PTCs in BXSB and Yaa mice at 24 wks of age, as shown by immunofluorescence. Normal distribution of $CD31^+$ PTC (arrows) in BXSB (A) and Yaa (B) mice kidney at 24 wks of age. Bars = 100μm.

(**C**) Number of $CD31^+$ PTCs in BXSB and Yaa mice kidneys at 24 wks of age. Values are mean ± s.e. Mann-Whitney *U*-test, n = 4.

(**D and E**) Distribution of PTC in Microfil-perfused thick kidney sections obtained from BXSB and Yaa mice at 24 wks of age. Normal distribution of PTC (arrows) in BXSB (D) and Yaa (E) mice kidneys.

AGN: autoimmune glomerulonephritis, PTC: peritubular capillary, BXSB: BXSB/MpJ, Yaa: BXSB/MpJ-*Yaa,* and wks: weeks.

Supplementary Figure 2

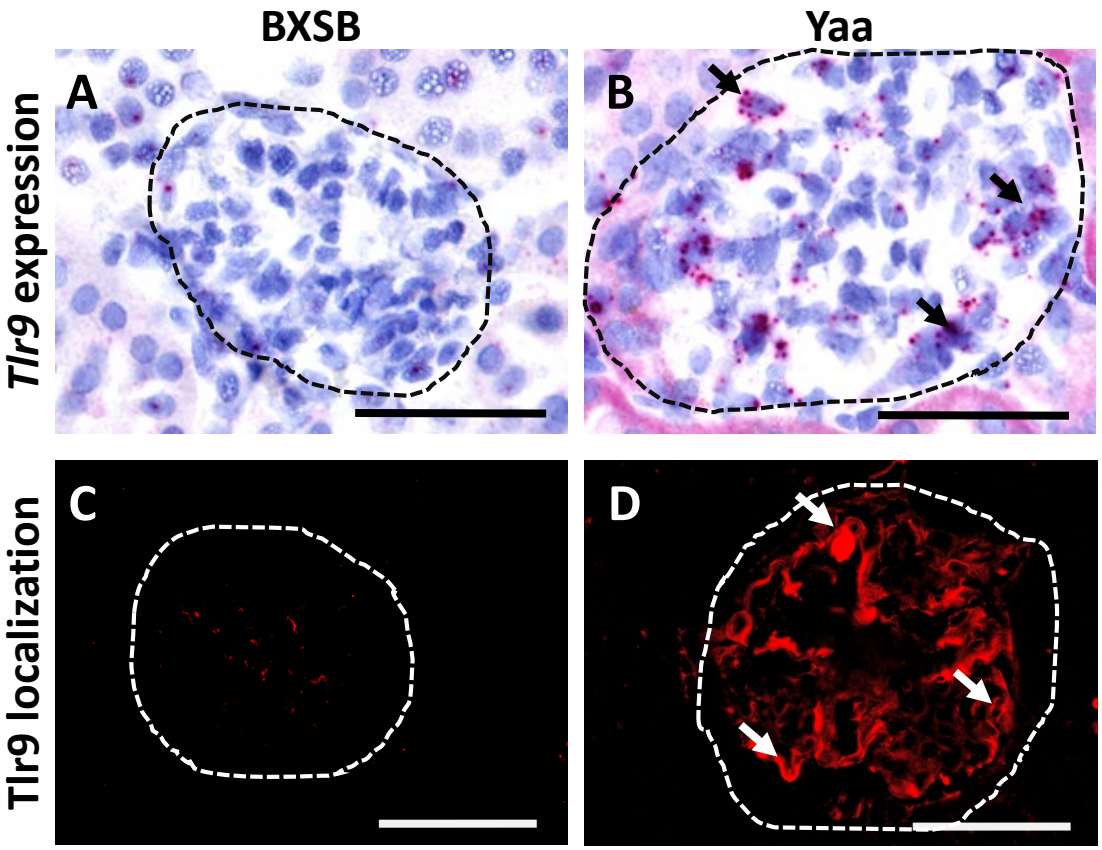

Supplementary Figure 2. *Tlr9* expression and localization in glomerulus of AGN model mice.

Tlr9 expression (black arrow) in glomerulus of BXSB (A) and Yaa (B) mice at 24 weeks of age. Tr9 protein localization (arrow) in the glomerulus of BXSB (C) and Yaa (D) mice at 24 weeks of age. Bars=50μm. AGN: autoimmune glomerulonephritis, BXSB: BXSB/MpJ and Yaa: BXSB/MpJ-*Yaa*

Supplementary Figure 3

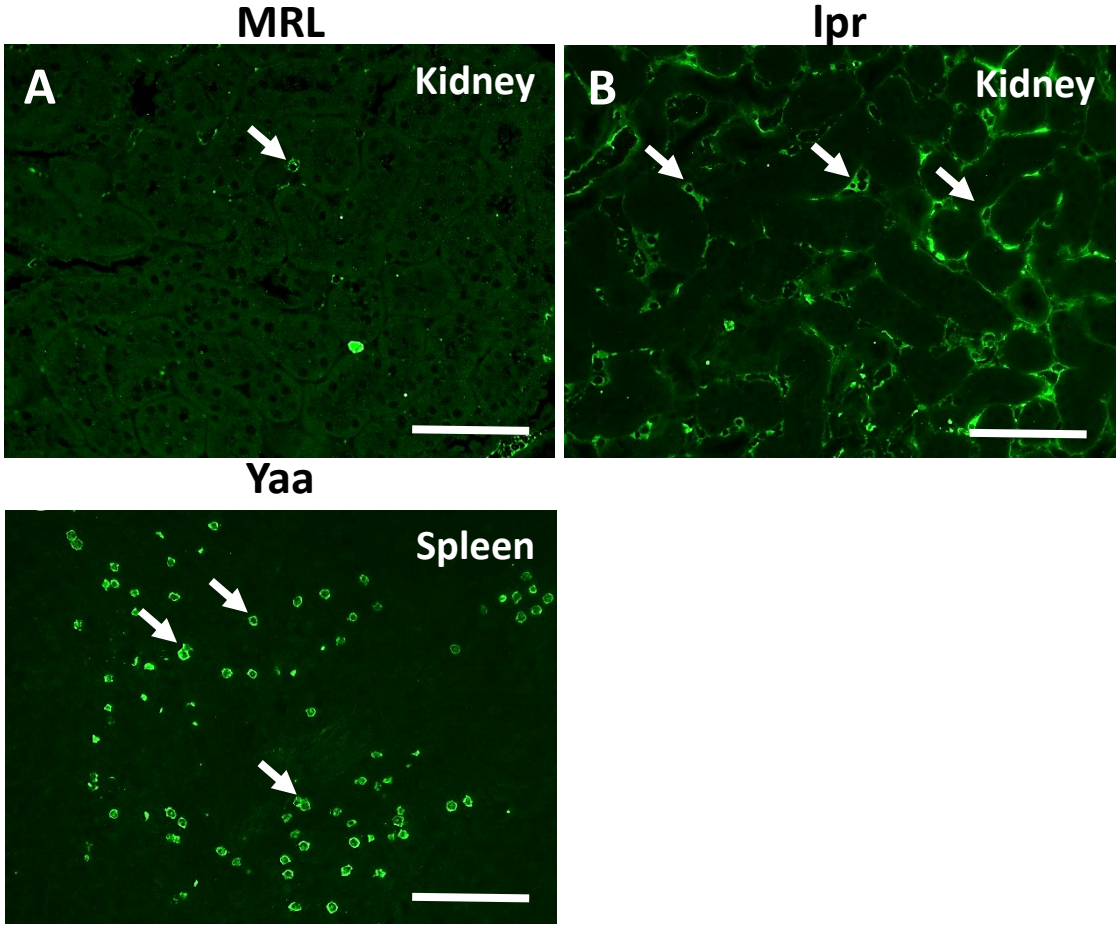

Supplementary Figure 3. Localization of Tlr9 in PTC and spleen.

Tlr9 protein localization (arrow) in the PTC of MRL/MpJ (A) and MRL/MpJ-*lpr* (B) mice at 24 weeks of age. Positive immunoreaction (arrow) also examined in spleen of Yaa mice at 24 weeks of age (C). Bars=100μm. MRL: MRL/MpJ, lpr: MRL/Mp-*lpr* and Yaa: BXSB/MpJ-*Yaa.*